VERSITA

CELLULAR & MOLECULAR BIOLOGY LETTERS
http://www.cmbl.org.pl

Received: 16 November 2011
Final form accepted: 18 April 2012
Published online: 19 April 2012

Volume 17 (2012) pp 349-375
DOI: 10.2478/s11658-012-0015-6

Research article

MODULATION OF PHYSIOLOGICAL AND PATHOLOGICAL ACTIVITIES OF LYSOZYME BY BIOLOGICAL MEMBRANES

VALERIYA TRUSOVA
Department of Biological and Medical Physics, V. N. Karazin Kharkov National University, 4 Svobody Sq., Kharkov 61077, Ukraine

Abstract: The molecular details of interactions between lipid membranes and lysozyme (Lz), a small polycationic protein with a wide range of biological activities, have long been the focus of numerous studies. The biological consequences of this process are considered to embrace at least two aspects: i) correlation between antimicrobial and membranotropic properties of this protein, and ii) lipid-mediated Lz amyloidogenesis. The mechanisms underlying the lipid-assisted protein fibrillogenesis and membrane disruption exerted by Lz in bacterial cells are believed to be similar. The present investigation was undertaken to gain further insight into Lz-lipid interactions and explore the routes by which Lz exerts its antimicrobial and amyloidogenic actions. Binding and Förster resonance energy transfer studies revealed that upon increasing the content of anionic lipids in lipid vesicles, Lz forms aggregates in a membrane environment. Total internal reflection fluorescence microscopy and pyrene excimerization reaction were employed to study the effect of Lz on the structural and dynamic properties of lipid bilayers. It was found that Lz induces lipid demixing and reduction of bilayer free volume, the magnitude of this effect being much more pronounced for oligomeric protein.

* Address for correspondence: Valeriya Trusova, 19-32 Geroyev Truda St., Kharkov 61144, Ukraine. E-mail: valtrusova@yahoo.com

Abbreviations used: CD – circular dichroism; CL – cardiolipin; DTT – dithiothreitol; DyL_{549} – DyLight 549; E/M – pyrene excimer-to-monomer intensity ratio; ESR – electron spin resonance; Fl – fluorescein; FRET – Förster resonance energy transfer; G+ – Gram positive bacteria; G– – Gram-negative bacteria; HLH – helix-loop-helix domain; IR – infrared; LPS – lipopolysaccharide; LUV – large unilamellar vesicles; Lz – lysozyme; PBS – phosphate buffered saline; PIE – pulse interleaved excitation; PC – phosphatidylcholine; PG – phosphatidylglycerol; PS – phosphatidylserine; $SeTau_{647}$ – SeTau-647-di-NHS; SLB – supported lipid bilayer; TIRFM – total internal reflection fluorescence microscopy; tr-FRET – time-resolved FRET

Key words: Amyloid toxicity, Antimicrobial activity, "Carpet" mechanism, Fluorescence spectroscopy, Lipid membranes, Lipid domain formation, Lysozyme, Membrane free volume, Membrane destabilization, Protein aggregation

INTRODUCTION

Lysozyme, a hydrolytic enzyme displaying antimicrobial, antitumor and immune modulatory activities, has long been the focus of extensive research efforts in numerous fields of inquiry. Discovered by Alexander Fleming in 1922, lysozyme was the first protein whose three-dimensional structure was characterized at atomic resolution [1]. Owing to its well-defined geometry and physicochemical properties Lz represents an attractive model in approaching a broad spectrum of fundamental problems including protein adsorption at interfaces [2], lipid-protein interactions [3-5], membrane fusion [6, 7], protein folding, aggregation and amyloid fibrillogenesis [8-10]. A number of studies provide evidence for pronounced lipid-associating ability of lysozyme [11-14]. Formation of Lz-lipid complexes is thought to be mediated by electrostatic forces between lipid anionic polar headgroups and positively charged protein amino acid residues, van der Waals interactions between lipid acyl chains and side groups of non-polar amino acids of Lz, hydrogen bonding between different lipid and protein moieties and a hydrophobic effect ensuring protein insertion into the membrane interior. The relative contributions of these binding components depend on a number of factors, including, in particular, milieu conditions (pH, ionic strength), lipid bilayer composition, physical state, surface distribution of its charge, etc. [15].

The biological significance of Lz-lipid complexation embraces at least two main aspects. The first one relates to the protein antibacterial activity. As part of an unspecific innate defense mechanism, Lz exerts its bactericidal action either independently by lysing the bacteria or as a component of a chain of biochemical and immunological reactions synergistically acting with nisin [16] or other antimicrobial peptides [17] to inactivate bacterial cells. The antibacterial activity of Lz is directed mainly against G+ bacteria. The main mechanism of cell lysis is the hydrolysis of the β(1→4) glycosidic bond between *N*-acetylglucosamine and muramic acid of the peptidoglycan layer in the bacterial cell wall promoting cell aggregation and loss of their viability [18, 19]. The specificity of Lz to G+ bacteria is explained by the fact that their peptidoglycan is freely accessible to lysozyme, contrary to G– bacteria, where the peptidoglycan layer is shielded by the LPS layer of the outer membrane [20]. However, this viewpoint is being intensively discredited by a growing body of evidence [21-24]. Accordingly, the occurrence of G– bacteria naturally sensitive to Lz [25] suggests that protein hydrolytic activity is not the only pathway of bacterial cell degradation. An increasing number of studies support the hypothesis of a non-enzymatic type of Lz antimicrobial action [21-24]. Specifically, it was shown that partially or

completely denatured protein with significantly reduced enzymatic activity or without it is capable of destroying not only G+, but also G– bacteria [24]. Similar to other peptides (e.g. cecropin, melittin, magainin, lactoferrin, protegrin, etc.) [26, 27], the properties, such as cationicity, hydrophobicity and amphipathicity, of lysozyme were supposed to be responsible for its membrane-disruptive ability and catalytically independent mechanism of antibactericidal action [20]. The specific amino acid sequences of Lz were shown to account for noncatalytic bacterial cell death differing from enzymatic lysis of membranes [28]. Particularly, Pellegrini and co-workers showed that cationic pentadecapeptide (amino acid residues 98–112) without muramidase activity, released from clostripain-digested Lz, possesses highly bactericidal action against both G+ and G– bacteria [24, 28]. This peptide is part of a helix-loop-helix domain (amino acid residues Asp_{87}–Arg_{114}) located at the upper lip of the Lz site cleft [24]. This finding is of special importance since an α-helical hairpin motif such as HLH is a common structural element of many bactericidal peptides including cecropin A and colicin E1 [29, 30]. Like other antimicrobial peptides, to reach its target (cytoplasmic membrane) Lz should penetrate the outer membrane of G– bacteria containing LPS or cross the outer cell wall of G+ bacteria containing acidic polysaccharides. While considering the action of antimicrobial peptides against G–microorganisms, Hancock et al. described this process as a self-promoted uptake pathway [31]. According to this mechanism, the peptides interact with the surface of LPS and partially neutralize it. This causes disruption of the outer membrane; peptides pass through it and reach the negatively charged phospholipid cytoplasmic membrane. Lz permeation of bacterial membrane was hypothesized to occur via a "carpet" mechanism proposed for antimicrobial peptides [24]. Briefly, this mechanism implies that Lz amphipathic α-helices, once adsorbed onto the bilayer surface, accumulate around themselves anionic lipids, thereby locally changing membrane curvature and composition. At the site of binding (i.e. within the region enriched in anionic lipids) the protein generates lateral pressure on the membrane, thus causing its invagination. This results in membrane thinning and uptake of some lipid molecules from the bilayer, followed by membrane deformation, defragmentation, micellization and finally cell death.

The second important implication of Lz-lipid interactions involves lysozyme fibrillogenesis. It is becoming generally accepted that aggregation of soluble proteins into highly ordered β-sheet fibrillar structures, termed amyloids, plays the cardinal role in etiology of a number of so-called conformational diseases, including Alzheimer's, Parkinson's and Huntington's diseases, type II diabetes, rheumatoid arthritis, and spongiform encephalopathies [32]. Accordingly, a causative link between lysozyme fibrillization and pathogenesis of systemic amyloidosis has been established [33]. A growing body of evidence from both theoretical and experimental studies suggests that protein aggregation requires the partial unfolding of the native state into aggregation-prone intermediate

transient conformation with the exposed hydrophobic regions, intermolecular contacts between which are responsible for oligomerization (Fig. 1) [34, 35].

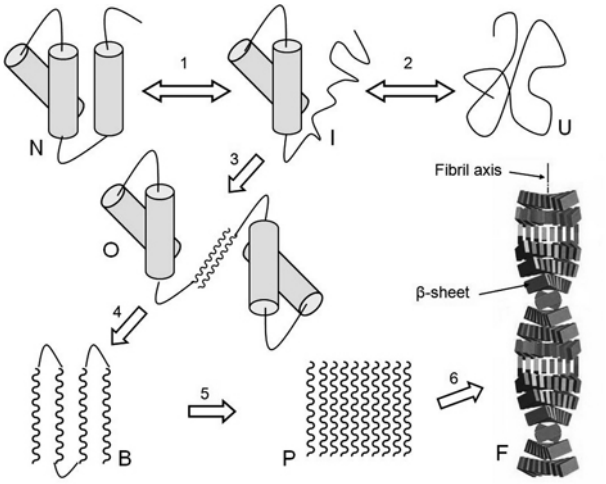

Fig. 1. Structural transformations of polypeptide chain: N – native state, I – partially unfolded conformation, U – fully unfolded conformation, O – protein oligomers with low content of β-sheets, B – β-sheet structure, P – pre-fibrillar aggregates, F – amyloid fibrils. β-sheets are depicted as wavy lines.

The factors facilitating protein unfolding and subsequent aggregation were proposed to involve milieu conditions (acidic pH, elevated temperature), the presence of organic solvents and denaturants or protein adsorption onto phospholipid surfaces such as monolayers or bilayers [36]. The crucial role of lipid/water interfaces in initiating and regulating the polypeptide self-association consists in providing a unique physicochemical environment which favors (i) the recruitment of protein molecules increasing thereby their local concentration necessary for oligomer nucleation, (ii) attenuation of electrostatic repulsion between charged monomers, (iii) destabilization of protein native structure, resulting in formation of aberrant unfolded states of polypeptide chain, (iv) peculiar alignment of protein molecules promoting their polymerization [37, 38]. Furthermore, ample evidence provides strong grounds for believing that lipid membranes represent a direct target for toxic pre-fibrillar protein aggregates which cause membrane distortion via formation of non-specific ionic channels and/or uptake of lipids into the forming fiber. An increasing number of reports support the hypothesis that seemingly unrelated processes such as protein aggregation and membrane disruption are strongly coupled phenomena [39]. Recent observations link directly lipid-assisted protein aggregation with membrane damage and subsequent toxicity of amyloid fibers. Selected examples in favor of this statement include membrane disruption by amyloid fibrils of islet amyloid polypeptide [40], Aβ-peptide [41], and temporins B and L [42], to name a few. The mechanisms by which amyloidogenic proteins exert a destructive

influence on membranes are supposed to be similar to those of antimicrobial peptides and include pore formation (toroidal and barrel-stave pores), nonspecific membrane permeabilization, detergent-like membrane dissolution, etc [39]. The above considerations imply that similar sequences of molecular events may underlie bactericidal and amyloidogenic actions of peptides and proteins, particularly lysozyme. Lz shares the properties of both antimicrobial and amyloidogenic peptides: it has an amphipathic helix, displays preferential affinity for anionic lipids, and the percentage of Lz helical structures increases upon protein binding to the lipid bilayer [43]. Furthermore, the finding that part of the amyloidogenic Lz fragment, involving amino-acid residues Gln_{57}–Ala_{107}, belongs to the above mentioned HLH structural motif of Lz, responsible for the protein-membrane association, provides additional support to the hypothesis of a correlation between antibacterial and amyloidogenic properties of Lz [9].

All these rationales strongly suggest that assessing the mechanisms of mutually dependent protein aggregation and membrane distortion is of utmost importance for understanding the protein biological functioning. Despite the great progress achieved in elucidation of general principles of Lz complexation with lipids, molecular pathways by which protein-lipid interactions govern structural perturbations of both protein and membrane still remain obscure. The present contribution, representing the quintessence of our studies on lysozyme-lipid interactions [44-46], is intended to fill at least partially this knowledge gap. More specifically, the main goals are: i) to analyze what factors are responsible for lipid-mediated transition of Lz into the aggregated state; and ii) to identify the molecular mechanisms by which Lz perturbs the structural integrity of the lipid bilayer. To achieve the above goals, different modifications of steady-state and time-resolved fluorescence spectroscopy were applied to yield in-depth information on Lz-membrane binding, protein conformational changes, protein-induced modification of lipid bilayer structure and the extent of Lz aggregation. Model lipid membranes were composed of zwitterionic lipid phosphatidylcholine and its mixtures with 5, 10, 20 or 40 mol% of anionic lipid phosphatidylglycerol (PG5, PG10, PG20 or PG40, respectively) or 5 and 25 mol% of cardiolipin (CL5 and CL25, respectively). The choice of PG and CL as anionic components of the examined model lipid systems was dictated by at least two reasons. The first one relates to the specificity of Lz interactions with CL and PG. Early ESR studies showed that among the anionic lipids, Lz has the highest affinity for CL and PG with protein selectivity decreasing in the order CL>PG>PS [47]. Second, CL and PG are constituents of bacterial membranes [48, 49] where Lz exerts its antimicrobial action.

MATERIALS AND METHODS

Materials

Chicken egg white lysozyme, fluorescein 5'-isothiocyanate (Fl), pyrene, HEPES and DTT were purchased from Sigma (St. Louis, MO). 1-palmitoyl-2-oleoyl-*sn*-

glycero-3-phosphocholine (PC), 1-palmitoyl-2-oleoyl-*sn*-glycero-3-phospho-*rac*-glycerol (PG) and bovine heart cardiolipin (CL) were from Avanti Polar Lipids (Alabaster, AL). Dimethyl sulfoxide was of Uvasol grade from Merck (Whitehouse Station, NJ). 2-(4,4-difluoro-5-methyl-4-bora-3a,4a-diaza-s-indacene-3-dodecanoyl)-1-hexadecanoyl-sn-glycero-3-phosphocholine (BODIPY-PC) was from Invitrogen (Carlsbad, CA), 1-(1,2-diacyl-sn-glycero-3-phospho)-3-{1′-[7-(4,4-difluoro-1,3,5,7-tetramethyl-4-bora-3*a*,4*a*-diaza-*s*-indacene-8-yl) heptanoyl]-2′-acyl-*sn*-glycero-3-phospho}-glycerol (BODIPY-CL) was synthesized as described in detail elsewhere [50]. 1-ethyl-3-[3-dimethylaminopropyl] carbodiimide hydrochloride (EDC), DyLight 549 (maleimide-activated form) and sodium borate buffer, pH 9, were provided by Thermo Fisher Scientific (Rockford, IL). PBS, pH 7.4, was from Amresco (Solon, OH). SeTau-647-di-NHS ($SeTau_{647}$) was provided by SETA BioMedicals (Urbana, IL).

Lysozyme labeling with fluorescent labels

Protein labeling with Fl. Reaction mixture containing equimolar amounts of Fl and Lz was prepared in 100 mM borate buffer. After incubation of the sample for 90 min at 25°C under continuous stirring in the dark, pH was adjusted to 7.4. Subsequently, the solution was dialyzed at 4°C against 20 mM HEPES, pH 7.4. The degree of labeling was estimated using extinction coefficients of 7.3×10^4 $M^{-1}cm^{-1}$ for Fl at 494 nm and 3.3×10^4 $M^{-1}cm^{-1}$ at 280 nm for Lz. Protein concentration was calculated after subtracting Fl absorbance using an extinction coefficient of 3.7×10^4 $M^{-1}cm^{-1}$ at 280 nm, and revealed a fluorescein-protein molar ratio of 1.76.

Protein labeling with DyLight 549. 0.5 mg of Lz was dissolved in 0.5 ml of 20 mM HEPES, pH 7.4, and subsequently mixed with DTT to reduce protein disulfide bonds. DTT:Lz molar ratio was 10:1. Afterwards, this mixture was incubated for 1.5 h with continuous stirring and dialyzed against 20 mM HEPES, pH 7.4 for 2 h. Reduced Lz solution was mixed with DyL_{549} prepared by dissolving 1 mg of the label in 1 ml of DMSO. This reaction mixture was incubated for 2 h at 37°C in the dark and then centrifuged at 14 000 g for 10 min. To ensure the complete separation of the free and protein-bound label, the supernatant was dialyzed against 20 mM HEPES, pH 7.4 overnight. Protein concentration and degree of labeling (D/P) were calculated spectrophotometrically by measuring the absorbance of conjugate at 280 and 562 nm, using extinction coefficients 3.3×10^4 $M^{-1}cm^{-1}$ at 280 nm and 1.5×10^5 $M^{-1}cm^{-1}$ at 562 nm for Lz and DyL_{549}, respectively. Calculated in such a way, protein concentration was found to be 75 μM and D/P was 0.35.

Protein labeling with SeTau-647-di-NHS. Stock solution of Lz was made by dissolving 1 mg of the protein in 1 ml of borate buffer, pH 9. Before preparation of the reaction mixture, functional groups of the label were additionally activated by dissolving 1 mg of $SeTau_{647}$ and 0.4 mg EDC in 1 ml of PBS, pH 7.4. Afterwards, protein solution and activated label were mixed and incubated with

continuous stirring for 6 h. After incubation, free and bound dyes were separated using Sephadex G25 columns. To prevent $SeTau_{647}$ degradation, all solutions were wrapped in foil and kept in the dark. Measuring the absorbance of conjugate at 280 and 650 nm, using extinction coefficients 3.3×10^4 $M^{-1}cm^{-1}$ at 280 nm and 3.7×10^5 $M^{-1}cm^{-1}$ at 650 nm for Lz and $SeTau_{647}$, respectively, yielded protein concentration and D/P of 15 μM and 0.15.

Preparation of lipid vesicles

LUV were made by the extrusion technique from PC and its mixtures with 5, 10, 20 and 40 mol% PG [51]. Appropriate amounts of lipid stock solutions were mixed in chloroform, evaporated to dryness under a gentle nitrogen stream, and then left under reduced pressure for 1.5 h to remove any residual solvent. The dry lipid films were subsequently hydrated with 20 mM HEPES, pH 7.4 at room temperature to yield lipid concentration of 1 mM. Thereafter, the samples were subjected to 15 passes through a 100 nm pore size polycarbonate filter (Millipore, Bedford, USA), yielding liposomes of the desired composition. Hereafter, liposomes containing 5, 10, 20 and 40 mol% PG are referred to as PG5, PG10, PG20 and PG40.

Preparation of supported lipid bilayers

Lipid vesicles from PC and its mixtures with 5 and 25 mol% CL were made by the extrusion technique [51]. BODIPY-PC or BODIPY-CL (0.3 mol% of total lipid, respectively) was added to the mixture of PC and CL prior to solvent evaporation. SLBs were made by vesicle fusion [52]. Homemade chambers, consisting of a glass frame to which two coverslips were attached using silicon grease, were used for microscopy. Chambers were filled with liposome suspension containing 100 μM total lipid and 5 mM $CaCl_2$, the latter added immediately before bilayer deposition. After incubation for 20 min in the dark, excess liposomes were thoroughly washed with working buffer. Immediately before bilayer formation, glass coverslips were cleaned by sonication for 30 min at 50°C with detergent solution, and rinsed with hot tap water, ethanol, and Milli-Q water. The slides and vesicles were used within 8 h after preparation. Hereafter, SLBs containing 5 or 25 mol% CL are referred to as CL5 or CL25.

Preparation of lysozyme fibrils

The reaction of lysozyme fibrillization was initiated using the approach developed by Holley and coworkers [53]. Protein solutions (3 mg/ml) were prepared by dissolving lysozyme in deionized water with subsequent slow addition of ethanol to a final concentration of 80%. Next, the samples were subjected to constant agitation at ambient temperature. Protein fibrillization kinetics were measured by monitoring the changes in Thioflavin T fluorescence at 483 nm.

Fluorescence measurements

All measurements were performed at room temperature in 20 mM HEPES in 1-cm path-length quartz cuvettes. Steady-state fluorescence experiments were done

with a Varian Cary Eclipse spectrofluorimeter (Varian Inc.). Fluorescein excitation wavelength was 490 nm. Excitation and emission slit widths were set at 5 nm. Fluorescence intensity measured in the presence of DyL_{549} at the maximum Fl emission (517 nm) was corrected for reabsorption and inner filter effects.

Time-resolved fluorescence measurements were carried out with a FluoTime200 fluorometer (PicoQuant GmbH) equipped with an ultrafast microchannel plate detector able to well resolve subnanosecond decays. A 470 nm pulsed laser diode (LDH-PC-470, PicoQuant GmbH) in the low-power regime (full width at half maxima for the pulse was < 70 ps) with 5 MHz repetition rates was used as an excitation source. The laser diode is routinely used to measure fluorescence decays and lifetimes within $\pm$ 10 ps accuracy. The lifetime data were analyzed by FluoTime software, version 4.0 (PicoQuant GmbH). For lifetime measurements, a monochromator supported by a long wave pass filter on the observation path was used. All the measurements for lifetime decay were performed using magic angle conditions.

Pyrene emission spectra were recorded with excitation wavelengths of 340 nm, and the excimer-to-monomer fluorescence intensity ratio (E/M) was determined by measuring fluorescence intensity at the monomer (392 nm) and excimer (468 nm) peaks.

PIE-FRET studies

Single-molecule experiments for Pulse Interleaved Excitation (PIE) were carried on a MicroTime 200 confocal fluorescence microscope system (PicoQuant GmbH, Germany). The pulsed excitation laser beams (470 nm for donor and 635 nm for acceptor) were directed by a dichroic mirror to a high numerical aperture (NA) water objective (60×, NA 1.2) and were focused 10 μm above the surface of the cover slip, into the sample volume. The collected fluorescence was split by a dichroic beam splitter (600DCXR, Chroma Technology) and spectrally filtered with emission bandpass filter 550/88 (Semrock) for the donor and a combination of long wavelength pass filters 647 and 650 (Semrock and Edmund Optics, respectively) for the acceptor. The emission was collected simultaneously by two avalanche photodiodes (MPD, PDM 1CTC) and processed by the PicoHarp300 time-correlated single-photon counting module. The lasers were each triggered with a repetition rate of 20 MHz and the 470 nm laser pulse was delayed by 25 ns with respect to the 635 nm laser. The integration time used to obtain the donor-acceptor time trace was 5 min. The data were analyzed with the SymPhoTime (version 5.0) software package that controlled the data acquisition as well. For the purpose of data analysis two decay curves obtained for donor and acceptor emission were analyzed separately [54]. The energy transfer efficiency E could be calculated as described earlier according to the formula:

$$E = \frac{F_{D_{ex}}^{A_{em}}}{F_{D_{ex}}^{A_{em}} + \gamma F_{D_{ex}}^{D_{em}}} \quad (1)$$

γ is a detection correction factor defined as:

$$\gamma = \frac{\phi_D \eta_D}{\phi_A \eta_A} \quad (2)$$

where $F_{D_{ex}}^{A_{em}}$ is the emission signal intensity of the acceptor after donor excitation, $F_{D_{ex}}^{D_{em}}$ is the emission signal intensity of the donor with donor excitation, η_D and η_A are donor and acceptor detection efficiencies, and ϕ_D and ϕ_A are quantum yields of donor and acceptor respectively. For our system with Fl working as a donor and SeTau647 as an acceptor detection correction was equal to 0.8.

Total internal reflection microscopy

Fluorescence from supported bilayers was observed using the inverted total internal reflection fluorescence microscope Olympus IX71 with an argon ion laser as an excitation source (excitation wavelength was 488 nm). High-resolution imaging was carried out with an oil immersion Olympus 60X TIRFM objective. Fluorescence images were collected using a Hamamatsu CCD camera interfaced to a computer and operated by Simple PCI software provided by the camera manufacturer. Subsequent image processing was performed using ImageJ software.

RESULTS

Analysis of mutually dependent processes of protein aggregation and membrane distortion was performed with a powerful set of fluorescence techniques. Fluorescence spectroscopy is one of the most widely used spectroscopic tools in the scope of lipid-protein interactions. While light scattering hampers CD measurements, Raman spectroscopy lacks sensitivity and water absorption affects IR spectra, fluorescence spectroscopy provides rapid, easily performed, extremely sensitive detection relatively independent of aforesaid processes which limit the use of the other spectroscopic techniques. Little or no damage to the examined matter, requirement of material micromolar concentration, relative simplicity in methodology, and involvement of relatively inexpensive instrumentation make fluorometry a broadly used research tool. Application of different variations of fluorescence spectroscopy such as fluorescent labeling, steady-state and time-resolved FRET, total internal reflection microscopy, and lifetime studies, allowed us to perform comprehensive examination of Lz-membrane complexation and to establish the correlation between protein aggregation and the impact of oligomeric protein on the membrane structure. Below, we will briefly overview the main experimental results and afterwards we will focus on a detailed discussion of the observed phenomena.

Lipid-assisted aggregation of lysozyme

Binding studies. To track the protein membrane binding lysozyme was covalently labeled with fluorescein (Fl), an environmentally sensitive

fluorophore. The complexation of tagged lysozyme with lipids manifested as a decrease of fluorescein emission at 514 nm (ΔI_{514}), presumably arising from the shift of equilibrium between fluorescent and non-fluorescent ionic forms of the label at the negatively charged lipid-water interface where pH is lowered compared to the bulk phase. Fluorescein emission displays a complex pH dependence, reflecting the equilibrium between the cation, neutral, monoanion and dianion ionic forms, of which only monoanion and dianion species are capable of fluorescing, with quantum yields being 0.37 and 0.93, respectively. In aqueous solution the pK_a values for stepwise fluorescein deprotonation are known to be approximately 2.1, 4.4, and 6.6 [55, 56]. Protonation of the dianionic form following the association of Fl-lysozyme with liposomal membranes is likely to be the reason for the observed fluorescence decrease. Notably, according to our estimates obtained in terms of the Gouy-Chapman double-layer theory, the lowest interfacial pH reached at PG content 40 mol% is approximately 5.2 (surface electrostatic potential is -126 mV, ionic strength 20 mM).

The monomer binding curves were obtained by monitoring the changes in Fl fluorescence as a function of lipid concentration and membrane content of anionic phospholipids. As seen from Fig. 2A, isotherms of Lz binding to neutral (PC) or weakly charged (PG5 and PG10) model membranes are characterized by a typical hyperbolic shape. Analysis of the obtained curves in terms of scaled particle theory (SPT)-based adsorption models accounting for electrostatic effects revealed that these isotherms can be described by a monomodal model (Eqs. (S1)-(S10) in Supplementary material at http://dx.doi.org/10.2478/s11658-012-0015-6) which suggests that upon binding to the lipid bilayer the protein retains its native globular conformation and monomeric state. In turn, association of Lz with highly charged lipid vesicles (PG20 and PG40) resulted in the conversion of binding isotherms from hyperbolic to sigmoidal with the steepness of the curves being increased with anionic lipid content (Fig. 2B).

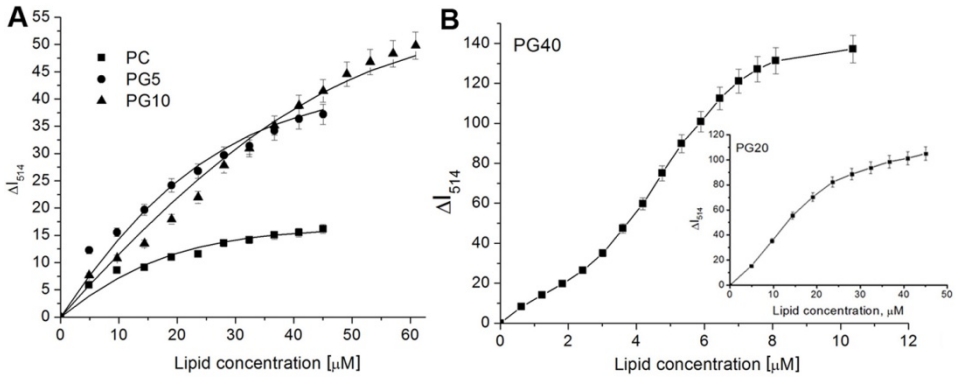

Fig. 2. Isotherms of lysozyme binding to the model membranes of different composition.

Neither the monomodal nor the multimodal adsorption model (Eq. (S19)-(S21) in Supplementary material at http://dx.doi.org/10.2478/s11658-012-0015-6),

which allows for the possibility of multiple interconvertible adsorbate conformations or protein association with membrane binding sites differing in their size and free energy of adsorption, was able to describe adequately the obtained results. Thus, we assumed that the sigmoidal form of the curves reflects the cooperativity of Lz-lipid binding, the most probable reason for which lies in formation of protein aggregates. In view of this, experimental data arrays were analyzed within the framework of two-state (Eq. (S11)-(S14), Supplementary) and cluster models (Eq. (S15)-(S18), Supplementary). The two-state model suggests that the adsorbed protein exists only in two states: as monomer and z_a-mer. Contrary to this, the cluster model considers highly heterogeneous populations of aggregated protein (i.e. protein clusters of arbitrary size and shape). It appeared that only the two-state model is applicable for successful description of the sigmoidal shape of the experimentally measured binding isotherms. This finding creates a basis for believing that Lz bound to PG20 and PG40 lipid membranes forms self-associates. It is also worth mentioning that the minimum degree of the protein oligomerization required to ensure sigmoidal shape of the binding curves was found to be 4, suggesting that tetramers represent a preferential form of Lz aggregates.

Time-resolved and single-molecule FRET. Advanced modifications of FRET, viz. time-resolved FRET (tr-FRET) and single-molecule pulse interleaved excitation FRET (PIE-FRET), were also applied to explore the impact of lipid bilayers on Lz self-association. The donor–acceptor pairs were represented by Fl and DyLight 549 (DyL_{549}) (tr-FRET studies) or Fl and SeTau-647-di-NHS (SeTau647) (PIE-FRET experiments), respectively, covalently attached to Lz. It is noteworthy at this point that the use of fluorescein as an energy donor is complicated by the aforementioned pH dependence of its fluorescence, giving rise to fluorescence intensity decrease upon Fl-Lz binding to negatively charged membranes with lowered interfacial pH. To account for this possibility, prior to performing tr-FRET and PIE-FRET measurements, Fl-Lz-lipid systems were allowed to attain the binding and protolytic equilibria during 30 min.

No FRET from Lz-Fl to Lz-DyL_{549} was observed in aqueous solution or in PC and PG5 lipid vesicles, as can be judged from unchanged fluorescence decay and corresponding lifetime of donor at increasing acceptor concentration (Fig. 3). Contrary to this, noticeable energy transfer was detected in the presence of PG10, PG20 and PG40 vesicles where elevating concentration of Lz- DyL_{549} resulted in reduction of Lz-Fl steady-state emission, appearance of the acceptor emission band in donor fluorescence spectra, and decrease in Lz-Fl lifetime and, consequently, relative quantum yield of the donor (Fig. 3). Furthermore, energy transfer was found to enhance at increasing PG molar fraction. When interpreting these data, it is important to bear in mind that the observed FRET can occur between either non-aggregated but closely located donor and acceptor, or aggregated protein species. To differentiate between these two cases, the obtained results were analyzed in terms of the 2D FRET model described by

Eqs. (S23)-(S26), Supplementary [44]. This model implies that if the cube of the logarithm of the ratio of donor deconvoluted intensities in the absence and presence of acceptor yields a straight line as a function of time, FRET arises from freely diffusing donors and acceptors [57, 58]. If this function deviates from linearity then FRET takes place between aggregated donors and acceptors.

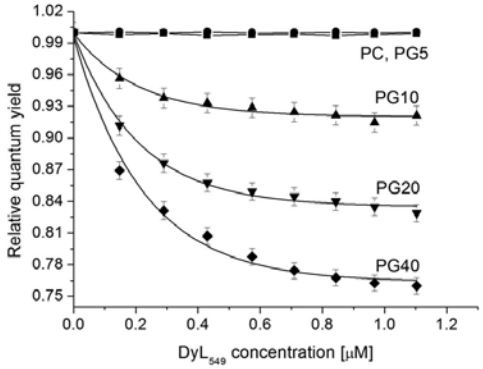

Fig. 3. The Profiles of resonance energy transfer between Fl and DyL_{549}, covalently attached to Lz, in different membrane systems.

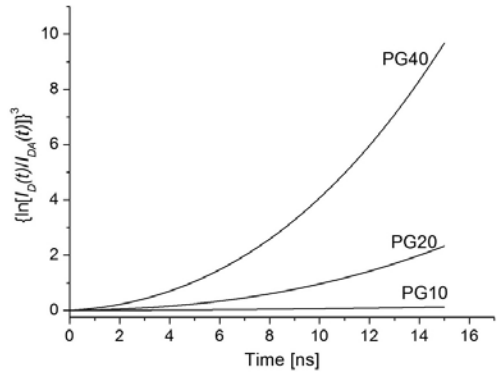

Fig. 4. Cubic form of logarithmic function ln $[I_D(t)/I_{DA}(t)]$ versus time. I_D and I_{DA} are Lz-Fl deconvoluted fluorescence intensities in the absence and presence of Lz-DyL_{549}, respectively.

As seen from Fig. 4, the curve is linear for Lz bound to PG10 liposomes and has a parabolic shape for the protein embedded into the PG20 and PG40 lipid bilayers. This finding assumes that upon association with weakly charged lipid membranes Lz retains its monomeric state while association with highly charged vesicles results in the formation of protein aggregates. Next, FRET profiles were quantitatively analyzed within the framework of the 2D FRET model obtained for protein oligomers and described in detail in the Supplementary material (Eqs. (S27)-(S31)). This model allows one to determine the parameters of protein self-association, such as degree of oligomerization (n), the distance

between monomers in protein assembly (R_a) and fraction of donors present in oligomers (X), from the results of time-resolved FRET studies [59]. However, when trying to approximate the experimental data by the above model we faced the problem of strong correlation between the calculated parameters. To perform more accurate data processing and to narrow the range of possible R_a values, an advanced modification of energy transfer called single-molecule PIE-FRET was applied. In contrast to traditional FRET where incomplete labeling, donor or acceptor photobleaching or other processes make an undesirable contribution to the measured energy transfer efficiency, PIE-FRET avoids the pollution by zero efficiency populations due to non-FRET phenomena [54, 60]. Briefly, in PIE-FRET both donor and acceptor are excited independently with two lasers. The laser pulses are delayed with respect to each other in order to produce a sequence with interleaved pulses. During the analysis of acquired data, the software extracts and subsequently analyzes only those pairs where an acceptor is present and its emission is solely due to energy transfer from a donor. Partially inactive FRET pairs which cause interfering artifacts in the standard FRET procedure are excluded. Application of such an approach to PG20 and PG40 systems revealed the existence of two subpopulations: low FRET species (averaged energy transfer efficiency is about 10%) and intermediate FRET species (averaged energy transfer efficiency is around 25%). The distance between donor and acceptor was found to fall in the range from 4 to 7 nm (Fig. 5).

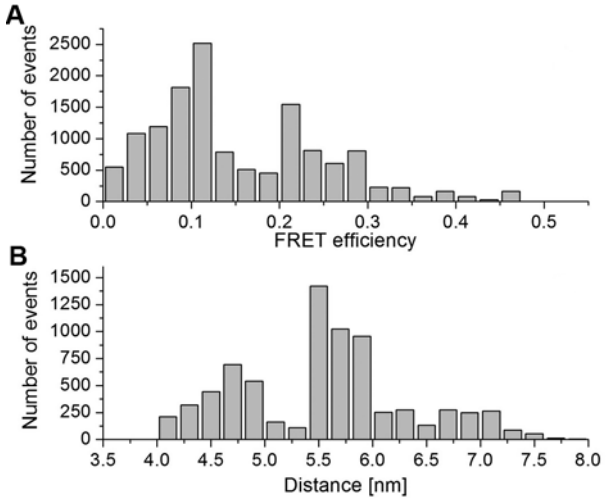

Fig. 5. PIE-FRET histograms of FRET efficiency (A) and distance (B) distributions in PG40 lipid membranes. Donor-acceptor pair was represented by Lz-Fl and Lz-SeTau$_{647}$.

These estimates for donor-acceptor separation were taken as the upper and lower limits of R_a during the analysis of tr-FRET results according to the above-mentioned model. Good agreement between theory and experiment was achieved with the set of parameters presented in Table 1. It is clearly seen from

the presented data that increasing content of anionic lipid PG resulted in the elevation of n and X, and reduction of R_a, reflecting the overall increase in Lz aggregation potential and tighter packing of monomers within the protein cluster.

Membrane perturbations induced by oligomeric lysozyme

Total internal reflection microscopy studies. To explore the effect of Lz on membrane integrity we first applied TIRFM of solid-supported lipid bilayers (SLBs). SLBs were composed of PC and its mixtures with 5 or 25 mol% of anionic lipid CL. To visualize the lipid bilayer structural changes evoked by Lz, SLBs contained trace amounts (0.3 mol% of total lipid) of fluorescent lipid, either BODIPY-PC (neat PC bilayers) or BODIPY-CL (CL-containing bilayers). In the absence of protein, freshly formed lipid bilayers were characterized by even fluorescence with no evidence of any bilayer defects (Fig. 6A).

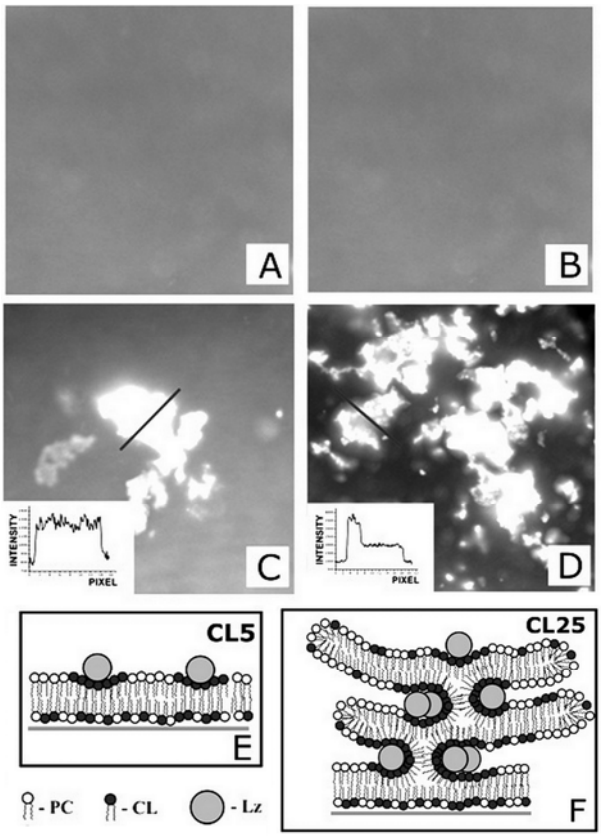

Fig. 6. Morphological changes of supported lipid bilayers induced by Lz. A, B – TIRFM images of PC solid-supported lipid bilayers in the absence (A) and presence (B) of Lz. C, D – Lz effect on the morphology of CL5 (C) and CL25 (D) SLBs. E, F – schematic representation of planar domain formation and multilayer stacking in supported lipid bilayers in response to lysozyme sorption.

Incorporation of Lz into neat PC membranes did not affect the lipid bilayer structure, as can be judged from invariance of BODIPY-PC fluorescence (Fig. 6B). In contrast, in CL-containing lipid bilayers protein binding caused rapid formation of large, well-defined areas with increased surface fluorescence of BODIPY-CL (Fig. 6C, D), the magnitude of the effect being dependent on CL content. The areas are of micrometer size, and in general remain in the plane of the SLB. These structures were not seen in control experiments in which plain buffer was added. Furthermore, to make sure that Lz itself does not contain any emitting moieties, increasing concentration of which could account for the observed expansion of bright spots, protein was incubated in working buffer over the glass substrate. It appeared that protein *per se* does not produce any fluorescent signal on the glass surface (data not shown). The above observations provide strong grounds for believing that the areas with increased surface fluorescence are induced exclusively by protein-lipid interactions. These areas seem to be formed by CL molecules assembling into domains upon Lz addition, because BODIPY-CL is the only fluorescing species excited by the laser source employed here. Analysis of the microscopy images with ImageJ software revealed that the area of lipid domains falls in the ranges 0.3-18.6 μm^2 and 0.34–21.4 μm^2 for CL5 and CL25 SLBs, respectively.

Another noteworthy observation is that at CL content 5 mol% the bright spots have more or less defined shape while in CL25 bilayers these spots represent a sort of irregular network of highly fluorescent fluid regions. The network seems to consist of bright regions embedded in a less fluorescent dark background which are characterized by a stepwise change in fluorescence intensity (Fig. 6D, inset). The step size between the areas of different intensity is discrete and approximately equals the intensity level of the parent bilayer (quantified after subtraction of camera noise). Intriguingly, intensity distribution profiles for CL5 SLBs were continuous, with brightness changes fluctuating around the average value (Fig. 6C, inset). This observation allowed us to hypothesize that Lz induces the formation of planar domains in CL5 bilayers (Fig. 6E), and more complex structures such as multilayers folded from the parent bilayer and stacked on it in CL25 membranes (Fig. 6F) [45]. These stacks represent sheets of lipid bilayers homogeneously stacked on top of each other and separated by protein molecules. Importantly, in stacking geometry electrostatic free energy of protein-membrane binding is likely to reach a minimum because all lipid charges are in contact with protein charges, while in the lamellar phase only a fraction of anionic lipids is vicinal to Lz. In CL5 SLBs, due to initially lower degree of demixing, the transition into 3D geometry is not required to reach a thermodynamic equilibrium, and planar domains enriched in either CL or PC represent the most stable membrane conformation. In attempting to explain the observed dependence of bilayer morphological changes on CL content in a parallel set of experiments we utilized TIRFM to record the isotherms of Lz sorption onto the examined SLBs. To achieve this goal, the protein was tagged with the Fl label. The results appeared to be similar to those

outlined in the Binding studies section; the binding curve was Langmuir-like for weakly charged CL5 bilayers and had a sigmoidal shape for CL25 SLBs (data not shown), suggesting that increasing electrostatic surface potential of the lipid bilayer promotes protein self-association. The above findings imply that aggregated Lz has a much more dramatic influence on membrane state compared to monomeric protein.

Pyrene excimerization studies. At the last step of our analysis of Lz-lipid relationships, the classical membrane probe pyrene was recruited to explore the effect of already pre-formed Lz oligomers on the physicochemical properties of the lipid bilayer. The reaction of Lz oligomerization was initiated as described in detail in the Materials and Methods section. The kinetics of protein fibrillization were measured by monitoring the changes in ThT fluorescence at 483 nm. Formation of Lz fibrils was characterized by an initial lag period (the first 8 days), as indicated by unchangeable ThT emission. Appearance of fibrillar aggregates was followed by significant increase in the dye fluorescence. The existence of Lz aggregates was verified by transmission electron microscopy.
As seen from Fig. 7, association of pre-aggregated protein with lipid vesicles brought about a decrease in the pyrene excimer-to-monomer intensity ratio (E/M), the magnitude of this effect being increased with PG content and protein concentration. The results obtained were rationalized in terms of the free volume model of diffusion in the lipid bilayer (for a detailed analysis see Supplementary material). Membrane free volume reflects the difference between the effective and van der Waals volumes of lipid molecules. Packing constraints and thermal motion may result in the enhanced *trans-gauche* isomerization of hydrocarbon chains and appearance of dynamic defects in the membrane interior. A local free volume arises from the lateral displacement of the hydrocarbon chain following kink formation. The free volume of the lipid bilayer depends on its composition, degree of acyl chain saturation, extent of hydration, temperature, etc. [61-63]. The free volume model considers diffusion of membrane constituents or guest molecules (such as pyrene monomers) as a three-step process*:* i) opening of a gap in a lipid monolayer due to formation of kinks in the hydrocarbon chains; ii) jumping of the diffusing molecule into a gap leading to the creation of a void; iii) occupation of the void by another solvent molecule. Decrease in E/M recovered upon Lz-lipid complexation suggests that incorporation of protein oligomers into the membrane interior induces the decrease in lipid bilayer free volume. Notably, monomeric Lz exerted a much less pronounced influence on pyrene spectral parameters and, consequently, on membrane structural properties. Furthermore, the magnitude of perturbations produced by protein oligomers was dependent on anionic lipid content. Thus, for example, at protein concentration 3.1 μM the decrease in E/M was ~18% for PC vesicles and ~24% for PG20 liposomes.

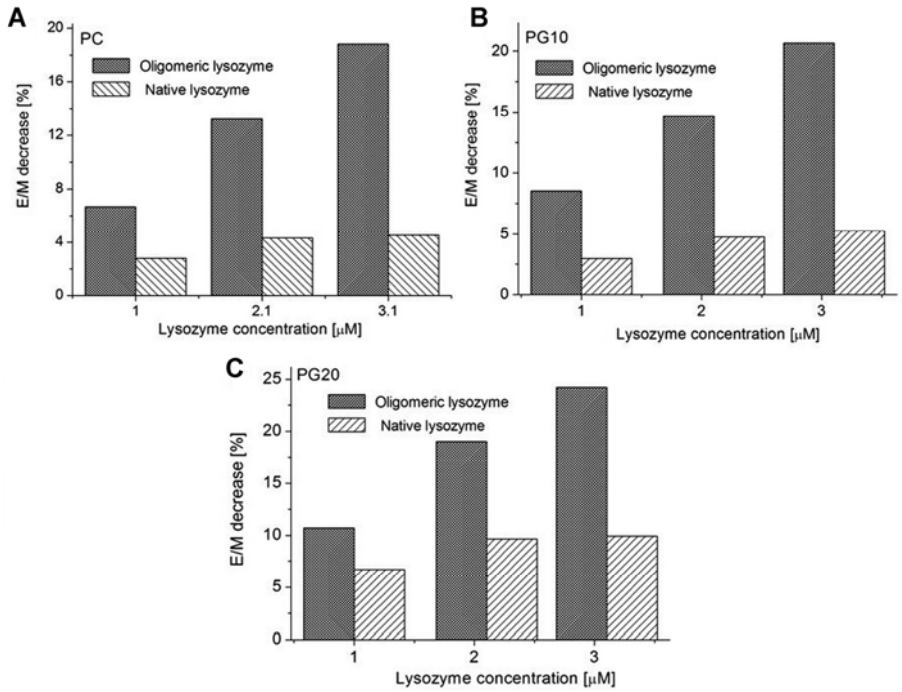

Fig. 7. Comparison of the effects produced by native and oligomeric Lz on the pyrene excimer-to-monomer intensity ratio in PC (A), PG10 (B) and PG20 (C) lipid membranes.

DISCUSSION

Lysozyme is a small polycationic protein discovered by Alexander Fleming in 1922 [64]. It was the first protein whose 3D structure was characterized at atomic resolution [65]. The name of this protein originates from two constituents highlighting the main biological functions of Lz – *lyso* due to its ability to lyse bacteria and *zyme* because of its enzymatic activity. Since its discovery and up to nowadays Lz has been the subject of an enormous number of studies. In the 1930s all research efforts were directed towards the exploration of molecular details of Lz enzymatic activity [66, 67]. As an enzyme, Lz catalyzes the hydrolysis of the β(1→4) glycosidic bond between the fourth carbon atom of *N*-acetylglucosamine and the first carbon atom of *N*-acetylmuramic acid of polysaccharide of the bacterial cell wall [19]. Carboxylic groups of deprotonated Asp_{52} and protonated Glu_{35} located in the active site of Lz participate in the reaction of hydrolysis. The breakage of the glycoside bond occurs due to the interactions between Asp_{52}, Glu_{35} and the atoms constituting this bond.

After the enzymatic properties of Lz had been studied in detail, researchers placed the mechanism of Lz antimicrobial action in the focus of scientific debates. A consensus could not be reached as to what represents the main target for Lz action – protoplasmic membrane, bacterial cell wall, or both.

Accordingly, Boasson concluded that Lz-induced lysis of bacteria is the result of modification of the cell wall structure [67]. In contrast, Meyer *et al.* hypothesized that Lz interactions with the mucoid structure of the membrane are crucial for the bacterial cells [66]. Epstein and Chain, in turn, conjectured that Lz attacks the polysaccharide of cell membranes [68]. Despite some contradictions, these early studies were based on the idea that Lz enzymatic properties underlie its antimicrobial action. The scientific world did not dispute this theory for about 50 years until the revolutionary works of Ibrahim *et al.* and Pellegrini *et al.* in the 1990s in which the authors showed that that Lz bactericidal properties are not always related to its enzymatic activity [28, 69]. These works opened a new epoch in Lz investigation and shifted the research towards a search for the mechanism which would explain the catalytically independent bactericidal action of the protein. A number of important conclusions were reached in the following decade. Thus, for example, the specific peptides have been isolated from inactivated Lz and reported to exhibit strong antimicrobial activity against both G+ and G– bacteria [70]. The penetration of the specific HLH domain, embracing the amino acid residues Asp_{87} – Arg_{114}, into the lipid bilayers and subsequent disruption of membrane integrity have been demonstrated to be responsible for the bactericidal activity of Lz [24]. Furthermore, Lz antimicrobial action has been shown to be enhanced by modifying the charge and hydrophobicity of the protein [10, 28]. In addition, Lz partially unfolded by heat treatment proved to exert catalytically independent antimicrobial action against both G+ and G– bacteria [24]. The enhancement of the bactericidal activity of lysozyme against Gram-negative bacteria was observed also after partial reduction of its disulfide bonds [71]. These results were interpreted in terms of the altered protein conformation minimizing the energetic cost of diffusion through the outer membrane of G– bacteria and enhanced insertion into the inner membrane. Overall, the main conclusion emerging from the cumulative results of these studies is that Lz antimicrobial action is catalytically independent and determined by membrane disruption properties of the protein HLH structural motif. Parallel to assessing the molecular details of Lz bactericidal action not connected with its enzymatic properties, in 1993 a study by Pepys *et al.* established another landmark in Lz science related to protein amyloidogenesis [33]. In this study the correlation between the accumulation of highly ordered Lz aggregates with a core β-sheet structure (amyloid) in human tissues and the development of such a debilitating disease as systemic amyloidosis was established. In view of this, all research efforts have been turned towards identification of the factors responsible for the conversion of Lz from the monomeric to the oligomeric state. A vast number of studies have been conducted and the principal role of gene mutations and oxidative and/or heat stress in promoting the protein aggregation has been established [38]. However, these findings could not fully explain the mechanism of amyloid cytotoxicity. The situation changed with the publication of a paper by Zhao *et al.* in which lipid-protein interactions were reported to represent the

major determinant of protein fibrillization [72]. Importantly, the same conclusion has been reached also for other amyloid-forming proteins, suggesting that the ability of the lipid bilayer to trigger polypeptide self-association is not limited only to Lz [73-75]. The problem of membrane-mediated protein aggregation has been addressed in a good wealth of both theoretical and experimental studies, and a common conclusion has been reached: on one hand, the lipid bilayer acts as a template for protein oligomer nucleation and growth, while on the other hand, the membrane represents the direct target for oligomeric structures which perturb lipid bilayer integrity, eventually causing cell death [37, 39]. The dual role of the membrane in the protein aggregation process and the finding that the mechanism of amyloid toxicity is similar to that of antimicrobial peptides resulted in a question being posed: are lipid-assisted protein aggregation and membrane disruption strongly coupled phenomena that represent links of the same chain? If this is the case, then one may expect that the sequence of events lying behind Lz amyloidogenesis and antimicrobial action is similar and involves the following: lipid-mediated protein aggregation → membrane destabilization induced by protein oligomers → cell death. Additional support for this statement comes from the studies of Huang and Chen *et al.*, where it was shown that antimicrobial peptides exist in two states: active aggregated state I where peptide oligomers distort the membrane by creating transbilayer pores which are fatal for cell viability, and inactive monomeric state S where the peptides do not influence membrane stability [76, 77]. These results indicate that protein aggregation may represent a necessary prerequisite for the peptide/protein destructive effect on the membrane.

In the present study we attempted to gain insight into the intricate interplay between Lz aggregation induced by protein binding to the lipid bilayer, and membrane distortion. Comprehensive analysis of Lz adsorption onto the lipid bilayer surface and intermolecular FRET between the fluorescent labels covalently attached to Lz revealed that Lz retains its native monomeric conformation in buffer or when bound to PC, PG5 and PG10 lipid vesicles. In contrast, elevating PG content up to 20 or 40 mol% brought about Lz transition to the oligomeric state. TIRFM experiments coupled with pyrene excimerization studies revealed that Lz substantially perturbs the structure of the lipid bilayer, leading to the formation of lipid domains and a decrease in membrane free volume, with the effect being much more pronounced for oligomeric protein.

In the most general case, enhancement of protein aggregation propensity in the presence of lipid membranes is attributed to the polypeptide conformational changes consistent with loosening of its tertiary structure and partial unfolding [36]. A growing body of evidence supports the idea that the lipid bilayer lowers the activation energy barrier for protein unfolding, providing an environment with reduced pH and a decreased dielectric constant whose concerted action enhances side chain charge repulsion and thereby gives rise to a more open structure with exposed aggregation-prone areas [35, 36]. Indeed, according to our estimates the pH decrease compared to the bulk phase (pH 7.4) can be as

large as 0.6, 1, 1.6 and 2.2 pH units for PG5, PG10, PG20 and PG40 vesicles, respectively. However, Lz is a very stable protein whose secondary and tertiary structures were shown to be virtually unperturbed even at $pH = 0.6$ [78]. Thus, we concluded that reduced interfacial pH is unlikely to be the main determinant of protein aggregation in a membrane environment. In seeking a mechanism that would explain the increasing oligomerization potential of Lz with PG fraction, one should pay attention to a large group of theoretical studies unraveling the nature of membrane-mediated protein-protein interactions [79-81]. These studies suggest that the main pathway for protein self-association is the long-range membrane-mediated attraction between the bilayer inclusions (proteins) arising from the overlap of membrane perturbations imposed by two neighboring inclusions. Speaking in more detail, when perturbed lipid annuli around the neighboring protein monomers overlap, attractive protein-protein interactions become energetically favorable, tending to minimize the overall free energy of protein-induced lipid bilayer deformations. Membrane deformations may include electrostatically controlled lipid demixing, implying the accumulation of oppositely charged lipids within the protein-membrane interaction zone, or elastic bilayer perturbations caused by hydrophobic mismatch and/or changes in the lipid order parameter, bilayer thickness and area per lipid molecule [81]. These perturbations create the gradient of bilayer parameters across the boundary of the protein adsorption site and produce positive line energy proportional to the circumference length of the protein-lipid interaction zone, favoring attractive interactions between the proteins because the circumference of two adjoining molecules is smaller than that of two isolated ones [82]. The results of our experiments are in good harmony with this scenario. Evidently, due to the initially lower degree of Lz binding to neutral and weakly charged lipid membranes compared to highly charged bilayers, the protein lateral density is relatively small and the frequency of the protein-induced membrane defects (e.g., formation of lipid domains) per unit area is low and insufficient for lipid annuli to overlap. Elevation of the anionic lipid fraction increases the concentration of bound protein and, consequently, its lateral density, thereby decreasing the distance between the adsorbed monomers. This results in an increased number of protein-induced membrane deformations per unit area, ensuring the juxtaposition of perturbed lipid annuli and aggregation of bound protein. The proposed mechanism readily explains the increase in the size of lipid domains with anionic lipid content revealed by TIRFM. Due to higher charge and circumference, Lz oligomers would enhance the demixing potential of CL, and trigger the formation of anionic lipid assemblies with a higher radius of curvature compared to monomer-induced domains. Apparently, under the conditions of elevated negative curvature strain, imposed by Lz assemblies, in-plane domains cannot provide the minimal free energy of the composite protein-lipid membrane, and the route by which the system further reduces the interaction energy seems to involve transformation of regular domains into multilayer stacks. Likewise, the results of pyrene excimerization studies

provided strong evidence that oligomeric Lz species affect membrane stability to a larger extent than protein monomers. Pyrene is a hydrophobic membrane probe highly sensitive to the structural and dynamic properties of a lipid bilayer. Pyrene excimerization is generally considered as a diffusion-controlled process reflecting the changes in membrane free volume. The revealed reduction in the bilayer characteristics produced by Lz may be interpreted in terms of the decreased rate of *trans-gauche* isomerization and ordering of hydrocarbon chains due to the protein's embedment into the membrane non-polar region. In this case, due to the larger size, Lz aggregates would decrease membrane free volume to a higher extent than monomeric species, leading to more significant ordering of lipid molecules.

Summarizing the results outlined here, the sequence of molecular events underlying Lz amyloidogenesis and antimicrobial activity seems to be as follows. The initial step is protein adsorption onto the surface of the lipid bilayer initiated by electrostatic attraction between oppositely charged Lz and phospholipid headgroups. The result of this stage of protein-lipid complexation is partial neutralization of the surface charge of both Lz and the lipid bilayer, and change in membrane curvature and surface pressure. The second stage involves several inter-connected processes: i) destabilization of Lz structure and exposure of hydrophobic regions on the protein surface, ii) increase in coverage of membrane surface with protein monomers, iii) aggregation of membrane-bound Lz. The final phase is global perturbations of the lipid bilayer by oligomeric protein involving membrane invagination, thinning and uptake of some lipid molecules from the bilayer. This gives rise to membrane deformation, defragmentation, micellization and eventually cell death. The described model is in accord with the "carpet" mechanism of antimicrobial peptide action. This finding corroborates the results of Ibrahim *et al.*, who also supposed that Lz causes damage to bacterial membranes via the "carpet" mechanism rather than according to the "pore" model [24]. Obviously, whereas membrane distortion induced by monomeric protein is not crucial yet for cell functioning, protein oligomers induce destabilization of the lipid bilayer to such an extent that the membrane completely loses its native structure and morphology, leading thereby to cell death. While the proposed mode of Lz action is auspicious from the viewpoint of antimicrobial activity because the protein kills the bacteria in such a way, accumulation of Lz oligomers and their destructive effect on membrane integrity in healthy tissues become lethal since they lead to the development of systemic amyloidosis. The present results may be of utmost importance when creating novel antimicrobial pharmaceuticals based on Lz as well as for the development of novel anti-amyloid strategies.

Acknowledgements. The author is sincerely grateful to Prof. Galyna Gorbenko for support and helpful discussions on the topic of the manuscript, Profs. Paavo Kinnunen, Zygmunt and Ignacy Gryczynski for providing the laboratory facilities, Dr. Irina Akopova for help with the TIRFM experiments and Dr. Rafal Luchowski for help with the PIE-FRET measurements.
This work was supported by the Science and Technology Center in Ukraine (grant number 4534), the Fundamental Research State Fund (grant number F28.4/007), and a short-term fellowship from the Human Frontier Science Program.

REFERENCES

1. Walsh, M.A., Schneider, T.R., Sieker, L.C., Dauter, Z., Lamzin, V.S. and Wilson, K.S. Refinement of triclinic hen-egg white lysozyme at atomic resolution. **Acta Cryst.** D54 (1998) 522-546.
2. Wertz, C.F. and Santore, M. Adsorption and reorientation kinetics of lysozyme on hydrophobic surfaces. **Langmuir** 18 (2002) 1190-1199.
3. Kimelberg, H.K. Protein-liposome interactions and their relevance to the structure and function of cell membranes. **Mol. Cell. Biochem.** 10 (1976) 171-190.
4. Zschornig, O., Paasche, G., Thieme, C., Korb, N., Fahrwald, A. and Arnold, K. Association of lysozyme with phospholipid vesicles is accompanied by membrane surface dehydration. **Gen. Physiol. Biophys.** 19 (2000) 85-101.
5. Zschornig, O., Paasche, G., Thieme, C., Korb, N. and Arnold, K. Modulation of lysozyme charge influences interaction with phospholipid vesicles. **Colloids Surf. B Biointerfaces** 42 (2005) 69-78.
6. de Arcuri, B.F., Vechetti, G.F., Chehin, R.N., Goni, F.M. and Morero, R.D. Protein-induced fusion of phospholipid vesicles of heterogeneous sizes. **Biochem. Biophys. Res. Commun.** 262 (1999) 586-590.
7. Posse, E., de Arcuri, B.F. and Morero, R.D. Lysozyme interactions with phospholipid vesicles: relationships with fusion and release of aqueous content. **Biochim. Biophys. Acta** 1193 (1994) 101-106.
8. Merlini, G. and Bellotti, V. Lysozyme: a paragmatic molecule for the investigation of protein structure, function and misfolding. **Clin. Chim. Acta** 357 (2005) 168-172.
9. Frare, E., Polverino de Laureto, P., Zurdo, J., Dobson, C. and Fontana, A. A highly amyloidogenic region of hen lysozyme. **J. Mol. Biol.** 340 (2004) 1153-1165.
10. Sato, T., Mattison, K.W., Dubin, P.L., Kamachi, M. and Morishima, Y. Effect of protein aggregation on the binding of lysozyme to pyrene-labeled polyanions. **Langmuir** 14 (1998) 5430-5437.
11. Tsunoda, T., Imura, T., Kadota, M., Yamazaki, T., Yamauchi, H., Kwon, O., Yokoyama, S., Sakai, H. and Abe, M. Effects of lysozyme and bovine serum

albumin on membrane characteristics of dipalmitoylphosphatidylglycerol liposomes. **Colloids Surf. B Biointerfaces** 20 (2001) 155-163.
12. Dimitrova, M.N., Matsumura, H., Terezova, N. and Neytchev, V. Binding of globular proteins to lipid membranes studied by isothermal titration calorimetry and fluorescence. **Colloids Surf. B Biointerfaces** 24 (2002) 53-61.
13. Ioffe, V.M. and Gorbenko, G.P. Lysozyme effect on structural state of model membranes as revealed by pyrene excimerization studies. **Biophys. Chem.** 114 (2005) 199-204.
14. Ioffe, V.M., Gorbenko, G.P., Deligeorgiev, T., Gadjev, N. and Vasilev, A. Fluorescence study of protein-lipid complexes with a new symmetric squarylium probe. **Biophys. Chem.** 128 (2007) 75-86.
15. Bergers, J.J., Vingerhoeds, M.H., van Bloois, L., Herron, J.N., Jassen, L.H., Fisher, M.J. and Crommeli, D. The role of protein charge in protein-lipid interactions. pH-dependent changes of the electrophoretic mobility of liposomes through adsorption of watersoluble, globular proteins. **Biochemistry** 32 (1993) 4641-4649.
16. Mastromatteo, M., Lucera, A., Siniqaqlia, M. and Corbo, M.R. Synergetic antimicrobial activity of lysozyme, nisin, and EDTA against Listeria monocytigenes in ostrich meat patties. **J. Food Sci.** 75 (2010) M422-M429.
17. Yan, H. and Hancock, R.E.W. Synergistic interactions of mammalian antimicrobial defense peptides. **Antimicrob. Agents Chemother.** 45 (2001) 1558-1560.
18. Kasprzewska, A. Plant chitinases – regulation and function. **Cell. Mol. Biol. Lett.** 8 (2003) 809-824.
19. Salton, M.R.J. The properties of lysozyme and its action on microorganisms. **Microbiol. Mol. Biol. Rev.** 21 (1957) 82-99.
20. Benkerroum, N. Antimicrobial activity of lysozyme with special relevance to milk. **Afr. J. Biotechnol.** 7 (2008) 4856-4867.
21. Masschalck, B., Deckers, D. and Michiels, C.W. Lytic and nonlytic mechanism of inactivation of gram-positive bacteria by lysozyme. **J. Food Prot.** 65 (2002) 1916-1923.
22. Bera, A., Biswas, R., Herbert, S., Kulauzovic, E., Weidenmaier, C., Peschel, A. and Götz, F. Influence of wall teichoic acid on lysozyme resistance in *Staphylococcus aureus*. **J. Bact.** 189 (2007) 280-283.
23. Hunter, H.N., Jing, W., Schibli, D.J., Trinha, T., Park, Y., Kim, S.C. and Vogel, H.J. The interactions of antimicrobial peptides derived from lysozyme with model membrane systems. **Biochim. Biophys. Acta** 1668 (2005) 175-189.
24. Ibrahim, H.R., Thomas, U. and Pellegrini, A. A helix-loop-helix peptide at the upper lip of the active site cleft of lysozyme confers potent antimicrobial activity with membrane permeabilization action. **J. Biol. Chem.** 276 (2001) 43767-43774.
25. Ellison, R.T. and Giehl, T.J. Killing of gram-negative bacteria by lactoferrin and lysozyme. **J. Clin. Invest.** 88 (1991) 1080-1091.

26. Hancock, R.E.W. and Chapple, D.S. Peptide antibiotics **Antimicrob. Agents Chemother.** 43 (1999) 1317-1323.
27. Keller, R.C.A. The prediction of novel multiple lipid-binding regions in protein translocation motor proteins: a possible general feature. **Cell. Mol. Biol. Lett.** 16 (2011) 40-54.
28. Pellegrini, A., Thomas, U., Bramaz, N., Klauser, S., Hunziker, P. and von Fellenberg, R. Identification and isolation of a bactericidal domain in chicken egg white lysozyme. **J. Appl. Microbiol.** 82 (1997) 372-378.
29. Silvestro, L. and Axelsen, P.H. Membrane-induced folding of cecropin A. **Biophys. J.** 79 (2000) 1465-1477.
30. Lindeberg, M., Zakharov, S.D. and Cramer, W.A. Unfolding pathway of the colicin E1 channel protein on a membrane surface. **J. Mol. Biol.** 295 (2000) 679-692.
31. Hancock, R.E.W. Peptide antibiotics. **Lancet** 349 (1997) 418-422.
32. Dobson, C.M. The structural basis of protein folding and its links with human disease. **Philos. Trans. Soc. Lond. Ser. B** 356 (2001) 133-145.
33. Pepys, M.B., Hawkins, P.N., Booth, D.R., Vigushin, D.M., Tennent, G.A., Soutar, A.K., Totty, N., Nguyen, O., Blake, C.C.F, Terry, C.J., Feest, T.G., Zalin, A.M. and Hsuan, J.J. Human lysozyme gene mutations cause hereditary systemic amyloidosis. **Nature** 362 (1993) 553-557.
34. Cao, A., Hu, D. and Lai, L. Formation of amyloid fibrils from fully reduced hen egg white lysozyme. **Protein Sci.** 13 (2004) 319-324.
35. Gorbenko, G.P. and Kinnunen, P.K.J. The role of lipid-protein interactions in amyloid-type protein fibril formation. **Chem. Phys. Lipids.** 141 (2006) 72-82.
36. McLaurin, J., Yang, D.S., Yip, C.M. and Fraser, P.E. Rewiew: modulating factors in amyloid-β-fibril formation. **J. Struct. Biol.** 100 (2000) 259-270.
37. Aisenbrey, C., Borowik, T., Byström, R., Bokvist, M., Lindström, F., Misiak, H., Sani, M. and Gröbner, G. How is protein aggregation in amyloidogenic diseases modulated by biological membranes? **Eur. Biophys. J.** 37 (2008) 247-255.
38. Zerovnik, E. Amyloid-fibril formation. Proposed mechanisms and relevance to conformational disease. **Eur. J. Biochem.** 269 (2002) 3362-3371.
39. Butterfield, S.M. and Lashuel, H.A. Amyloidogenic protein – membrane interactions: mechanistic insight from model systems. **Angew. Chem. Int. Ed.** 49 (2010) 5628-5654.
40. Sparr, E., Engel, M.F.M., Sakharov, D., Sprong, M., Jacobs, J., de Kruijf, B., Hoppener, J.W.M. and Killian, J.A. Islet amyloid polypeptide-induced membrane leakage involves uptake of lipids by forming amyloid fibers. **FEBS Lett.** 577 (2004) 117-120.
41. Arispe, N., Rojas, E. and Pollard, H. Alzheimer's disease amyloid beta protein forms calcium channels in bilayer membranes: blockade by tromethamine and aluminium. **Proc. Natl. Acad. Sci. USA** 89 (2003) 10940-10944.

42. Domanov, Y.A. and Kinnunen, P.K.J. Antimicrobial peptides temporins B and L induce formation of tubular lipid protrusions from supported phospholipid bilayers. **Biophys. J.** 91 (2006) 4427-4439.
43. Lippert, J.L., Lindsay, R.M. and Schultz, R. Laser-Raman investigation of lysozyme-phospholipid interactions. **Biochim. Biophys. Acta** 599 (1980) 32-41.
44. Trusova, V.M., Gorbenko, G.P., Sarkar, P., Luchowski, R., Akopova, I., Patsenker, L.D., Klochko, O., Tatarets, A.L., Kudriavtseva, Yu.O., Terpetschnig, E.A., Gryczynski, I. and Gryczynski Z. Forster resonance energy transfer evidence for lysozyme oligomerization in lipid environment. **J. Phys. Chem. B.** 114 (2010) 16773-16782.
45. Trusova, V.M., Gorbenko, G.P., Akopova, I., Molotkovsky, J.G., Gryczynski, I., Borejdo, J. and Gryczynski Z. Morphological changes of supported lipid bilayers induced by lysozyme: planar domain formation vs. multilayer stacking. **Colloids Surf. B.** 80 (2010) 219-226.
46. Gorbenko, G.P. and Trusova, V.M. Effects of oligomeric lysozyme on structural state of model membranes. **Biophys. Chem.** 154 (2011) 73-81.
47. Sankaram, M. and Marsh. D. Protein-lipid interactions with peripheral membrane proteins. In: **Protein-lipid interactions**, Elsevier, 1993, 127-162.
48. Filgueiras, M.H. and Op den Kamp, J.A. Cardiolipin, a major phospholipid of Gram-positive bacteria that is not readily extractable, **Biochim. Biophys. Acta** 620 (1980) 332-337.
49. Teuber, M. and Bader, J. Action of polymyxin B on bacterial membranes: phosphatidylglycerol- and cardiolipin-induced susceptibility to polymyxin B in *Acholeplasma laidlawii* B. **Antimicrob. Agents Chemother.** 9 (1976) 26-35.
50. Boldyrev, I.A., Zhai, X., Momsen, M.M., Brockman, H.L., Brown, R.E. and Molotkovsky, J.G. New BODIPY lipid probes for fluorescence studies of membranes. **J. Lipid Res.** 48 (2007) 1518-1532.
51. Mui, B., Chow, L. and Hope, M. Extrusion technique to generate liposomes of defined size. **Meth. Enzymol.** 367 (2003) 3-14.
52. Richter, R., Mukhopadhyay, A. and Brisson, A. Pathways of lipid vesicle deposition on solid surfaces: a combined QCM-D and AFM study. **Biophys. J.** 85 (2003) 3035-3047.
53. Holley, M., Eginton, C., Schaefer, D. and Brown, L.R. Characterization of amyloidogenesis of hen lysozyme in concentrated ethanol solution. **Biochem. Biophys. Res. Commun.** 373 (2008) 164-168.
54. Kapanidis, A.N., Lee, N.K., Laurence, T.A., Doose, S., Margeat, E. and Weiss, A. Fluorescence-aided molecule sorting: analysis of structure and interactions by alternating-laser excitation of single molecules. **Proc. Natl. Acad. Sci. USA** 101 (2004) 8936-8941.
55. Sjöback, R., Nygren, J. and Kubista, M. Absorption and fluorescence properties of fluorescein. **Spectrochim. Acta** A 51 (1995) L7-L21.

56. Kubica, K., Langer, M. and Gabrielska, J. The dependence of fluorescein-PE fluorescence intensity on lipid bilayer state. Evaluating the interaction between the probe and lipid molecules. **Cell. Mol. Biol. Lett.** 8 (2003) 943-954.
57. Wolber, P.K. and Hudson, B.C. An analytical solution to the Förster energy transfer problem in two dimensions. **Biophys. J.** 28 (1979) 197-210.
58. John, E. and Jähnig, F. Aggregation state of melittin in lipid vesicle membranes. **Biophys. J.** 60 (1991) 319-328.
59. Li, M., Reddy, L.G., Bennett, R., Silva, N.D., Larry, J., Jones, R. and Thomas, D.D. A fluorescence energy transfer method for analyzing protein oligomeric structure: application to phospholamban. **Biophys. J.** 76 (1999) 2587-2599.
60. Fore, S., Yuen, Y., Hesselink, L. and Huser, T. Pulsed-interleaved excitation FRET measurements on single duplex DNA molecules inside C-shaped nanoapertures. **Nano Lett.** 7 (2007) 1749-1756.
61. Montroll, E.W. Random walks on lattices. **J. Math. Phys.** 10 (1969) 753-765.
62. Galla, H.J., Hartmann, W., Theilen, U. and Sackmann, E. On two-dimensional random walk in lipid bilayers and fluid pathways in biomembranes. **J. Membr. Biol.** 48 (1979) 215-236.
63. Barenholz, Y., Cohen, T., Haas, E. and Ottolenghi, M. Lateral organization of pyrene-labeled lipids in bilayers as determined from the deviation from equilibrium between pyrene monomers and excimers. **J. Biol. Chem.** 271 (1996) 3085-3090.
64. Fleming, A. On a remarkable bacteriolytic element found in tissues and secretions. **Proc Roy. Soc. Ser. B** 93 (1922) 306-317.
65. Blake, C.C., Koenig, D.F., Mair, G.A., North, A.C., Phillips, D.C., and Sarma, V.R. Structure of hen egg-white lysozyme. A three-dimensional Fourier synthesis at 2 Angstrom resolution. **Nature** 206 (1965) 757-761.
66. Meyer, K., Palmer, J.W., Thompson, R. and Khorazo, D. On the mechanism of lysozyme action. **J. Biol. Chem.** 113 (1936) 479-486.
67. Boasson, E.H. On the bacteriolysis by lysozyme. **J. Immunol.** 34 (1938) 281-293.
68. Epstein, L.A. and Chain, E. Some observations on the preparation and properties of the substrate of lysozyme. **Brit. J. Exptl. Pathol.** 21 (1940) 339-355.
69. Ibrahim, H.R., Yamada, M., Matsushita, K., Kobayashi, K. and Kato, A. Enhanced bactericidal action of lysozyme to Escherichia coli by inserting a hydrophobic pentapeptide into its C terminus. **J. Biol. Chem.** 269 (1994) 5053-5063.
70. Hunter, H.N, Jing, W., Schibli, D.J., Trinha, T., Park, Y., Kim, S.C. and Vogel, H.J. The interactions of antimicrobial peptides derived from lysozyme with model membrane systems. **Biochim. Biophys. Acta** 1668 (2005) 175-189.

71. Touch, V., Hayakawa, S. and Saito, K. Relationships between conformational changes and antimicrobial activity of lysozyme upon reduction of its disulfide bonds. **Food Chem.** 84 (2004) 421-428.
72. Zhao, H., Tuominen, E.K.J. and Kinnunen, P.K.J. Formation of amyloid fibers triggered by phosphatidylserine-containing membranes. **Biochemistry** 43 (2004) 10302-10307.
73. Choo-Smith, L.P., Garson-Rodriges, W., Glabe, C.G. and Surewicz, W.K. Acceleration of amyloid fibril formation by specific binding of Aβ-(1-40) peptide to ganglioside-containing model membranes. **J. Biol. Chem.** 272 (1997) 22987-22990.
74. Morillas, M., Swietnicki, W., Gambetti, P. and Surewicz, W.K. Membrane environment alters the conformational structure of the recombinant human prion protein. **J. Biol. Chem.** 274 (1999) 36859-36865.
75. Zhu, M., Li, J. and Fink, A.L. The association of α-synuclein with membranes affects bilayer structure, stability and fibril formation. **J. Biol. Chem.** 278 (2003) 40186-4097.
76. Huang, H.W. Action of antimicrobial peptides: two-state model. **Biochemistry** 39 (2000) 8347-8352.
77. Chen, F.Y., Lee, M.T. and Huang, H.W. Sigmoidal concentration dependence of antimicrobial peptide activities: a case study of alamethicin. **Biophys. J.** 82 (2002) 908-914.
78. Polverino de Laureto, P., Frare, E., Gottardo, R., Van Dael, H. and Fontana, A. Partly folded states of members of the lysozyme/lactalbumin superfamily: a comparative study by circular dichroism spectroscopy and limited proteolysis. **Protein Sci.** 11 (2002) 2932-2946.
79. Lagüe, P., Zuckermann, M.J. and Roux, B. Lipid-mediated interactions between intrinsic membrane proteins: a theoretical study based on integral equations. **Biophys. J.** 79 (2000) 2867-2879.
80. Lagüe, P., Zuckermann, M.J. and Roux, B. Lipid-mediated interactions between intrinsic membrane proteins: dependence on protein size and lipid composition. **Biophys. J.** 81 (2001) 276-284.
81. Zemel, A., Ben-Shaul, A. and May, S. Membrane perturbation induced by interfacially adsorbed peptides. **Biophys. J.** 86 (2004) 3607-3619.
82. Denisov, G., Wanaski, S., Luan, P., Glaser, M. and McLaughlin, S. Binding of basic peptides to membranes produces lateral domains enriched in the acidic lipids phosphatidylserine and phosphatidylinositol 4,5-bisphosphate: an electrostatic model and experimental results. **Biophys. J.** 74 (1998) 731-744.